www.czasopisma.pan.pl PAN POLSKA AKADEMIA NAUK www.journals.pan.pl

DE GRUYTER OPEN

Arch. Min. Sci., Vol. 59 (2014), No 4, p. 869–886

Electronic version (in color) of this paper is available: http://mining.archives.pl

DOI 10.2478/amsc-2014-0060

GRZEGORZ KORTAS*, AGNIESZKA MAJ*

DEFORMATIONS OF THE PROTECTION SHELF IN THE "WAPNO" SALT MINE, BASED ON MODEL STUDIES

ODKSZTAŁCENIA PÓŁKI OCHRONNEJ W KOPALNI SOLI W WAPNIE NA PODSTAWIE BADAŃ MODELOWYCH

The catastrophic mine failure resulting from the inrush of water into the Wapno Salt Mine was probably caused by a fracture in the roof protection shelf. The purpose of the present study was to apply the method of the homogenization of the multi-level room-and-pillar structure in the Wapno Salt Mine for 3D+t modelling of the elastic-viscous medium to determine the distribution of stress and strain, and, on that basis, to estimate the geomechanical conditions existing in the roof shelf. This paper presents briefly the spatial development of the salt mine's structure and the results of the surveying measurements carried out during the salt mine's operation and after the mine was flooded. Those results constituted a basis for the verification of the introduced homogenization parameters, i.e. the time-dependent changes of the elasticity modulus and the susceptibility to creep at particular salt mine's levels. A simulated process demonstrated the development of positive values of principle stresses, increasing with time, and of omnidirectional tensile strains. In such conditions, the cracking of the protection shelf body could proceed, also with opening of water flow paths from the dome cap into the salt mine's workings. This paper presents a new research method, the results of its application, and the obtained distribution of stresses and strains that can be useful for the assessment of water hazard in other salt mines.

Keywords: salt dome, model studies, homogenization, protection shelf

Katastrofa górnicza wywołana wdarciem wody do kopalni soli w Wapnie spowodowana była prawdopodobnie pęknięciem ochronnej półki stropowej. Celem tej pracy było zastosowanie metody homogenizacji struktury komorowo-filarowej wielopoziomowej kopalni Wapno do modelowania ośrodka sprężysto-lepkiego 3D+t dla określenia rozkładu naprężeń i odkształceń oraz na tej podstawie oszacowania warunków geomechanicznych w półce stropowej. W pracy przedstawiono krótko rozwój przestrzenny struktury kopalni oraz wyniki przeprowadzonych pomiarów geodezyjnych w czasie działalności kopalni i po jej zatopieniu. Wyniki te były podstawą do weryfikacji wprowadzanych parametrów homogenizacji, tj. zmian w czasie modułu odkształceń i podatności na pełzanie poszczególnych poziomów kopani. Symulowany proces wykazał wykształcanie się rosnących w czasie dodatnich naprężeń głównych oraz

* STRATA MECHANICS RESEARCH INSTITUTE OF THE POLISH ACADEMY OF SCIENCES, UL. REYMONTA 27, 30-059 KRAKÓW, POLAND

wszechstronnych odkształceń rozciągających. W takich warunkach postępować mogło spękanie calizny półki ochronnej, a także otwieranie dróg przepływu wód z zawodnionej czapy wysadu do wyrobisk. W pracy przedstawiono nową metodę badań, jej wyniki i otrzymane rozkłady naprężeń i odkształceń, która może być zastosowana w ocenie zagrożenia wodnego kopalń soli.

Słowa kluczowe: wysad solny, badania modelowe, homogenizacja, półka ochronna

1. Introduction

The protection of underground salt mines against waters found in the formations that surround salt domes consists primarily in the maintenance of tight surroundings of the room-and-pillar structure by leaving protective shelf and pillars close to the salt dome boundaries. The tightness of pillars and protection shelves is also important for the purpose of underground liquid or gas storage in salt caverns (Ślizowski & Urbańczyk, 2012). The salt bodies are subjected to deformations which increase with time under the influence of workings. Such deformations are difficult to measure. Based on the symptoms of rock mass movements, a view was formulated, claiming that catastrophic inrush of water into the underground Wapno Salt Mine in 1977 could have been initiated by the tensile strain of the roof protection shelf (Kortas, 1979). Only the presently available research methods, applied to determine the influence of the mining workings on rock mass and land surface (e.g. Kortas, 2007; Tajduś, 2013), allow us to verify such hypotheses and use research results for an analysis of hazards in the locations displaying similar geological and mining conditions.

The purpose of this paper is to present a new method of determining deformations within the roof protection shelf, based on 3D+t model studies of the elastic-viscous medium, with the application of homogenization of the room-and-pillar structure in the Wapno Salt Mine, as well as to demonstrate that the hypothesis of the connection between the deformations occurring in the roof protection shelf with water inflow is also realistic in the case of the geological and mining conditions that are similar to those of the Wapno Salt Mine.

In this work, we have used the results of own research conducted under the project designed for the assessment of the safety status of post-mining areas in Wapno (Kortas & Maj, in: Rasała, 2014).

2. Symptoms of the Rock Mass Movement in the Wapno Salt Mine

The horizontal cross-section of the Wapno salt dome is similar to oval, with 900 m and 350 m axes. The salt dome cap is located under the Quaternary formations. It extends from the depth of ca. 160 m up to the central section of land surface. The exploitation Levels (III-X) were established under a 200 m roof protection shelf, with 50 m protection boundary pillars. At Levels I and II (within the roof protection shelf), and XI and XII, only main galleries were excavated, with single rooms at Level X in 1977. The 15 m wide pillars correspond to 15 m high rooms. Smaller 10 m high pillars were left at Level IV. Larger 20 m high rooms were excavated at Level IX. The distribution of rooms in the Salt Mine is presented in Fig. 1.

First, salt was extracted from Level IV in 1920-1939. Extraction started at Level III in 1943 and it was completed in 1968. In 1952-1968 salt was mined at Levels V and VI. Later, in

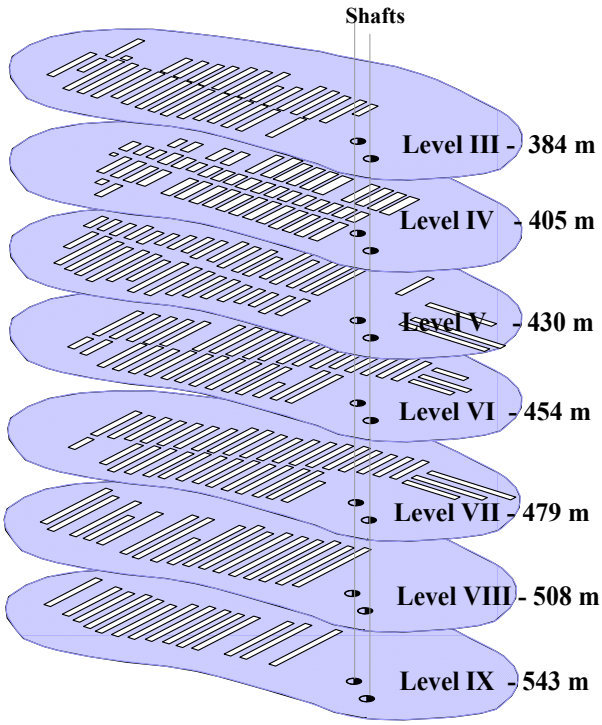

Fig. 1. The diagram of the distribution of rooms at Levels III-IX

1960-1972, extraction was continued in parallel at Levels VII, VIII and Level IX. In the 1970's, Levels XI and XII were made available and prepared for mining. However, protection pillars and shelves suffered deformations which were increasing with time. The most degraded were the pillars between rooms at Levels IV and V.

By the end of 1930's, surveyors started to measure land surface subsidence, while the measurements of vertical benchmark displacements in the salt mine's galleries started in the 1950's. Surveying observations inside the Salt Mine, initiated by S. Szpetkowski and carried out by J. Czajkowski, T. Malara, and L. Wesołowski, indicated the propagation of subsidence and uplifts, depending on the locations of underground workings at lower and upper levels, and those were changing with time (Fig. 2).

During the mining operations, the volumes of the working were regularly increasing, with limited increase of land subsidence rates (Fig. 3). The rate of maximum land subsidence at Level III reached –30 mm/year in 1961-1976, and that of land surface Benchmark 127 above: –16.2 mm/year. From 1973 to 1976, surveyors observed a regular trough at that level, displaying the maximum subsidence rate of –46 mm/year. Although the maximum land surface subsidence rate increased twice in the 1970's, up to –30 mm/year, it remained much slower than that at Level III. Consequently, the space containing the salt protection shelf and the salt dome cap was expanding in the vertical direction. Also, volumetric tensile strain of the rock mass were increasing, which was indicated by the estimated drop of the proportion of the subsidence volume to the workings' volume in the periods until 1945 and until 1977, by 0.090 and 0.037, respectively.

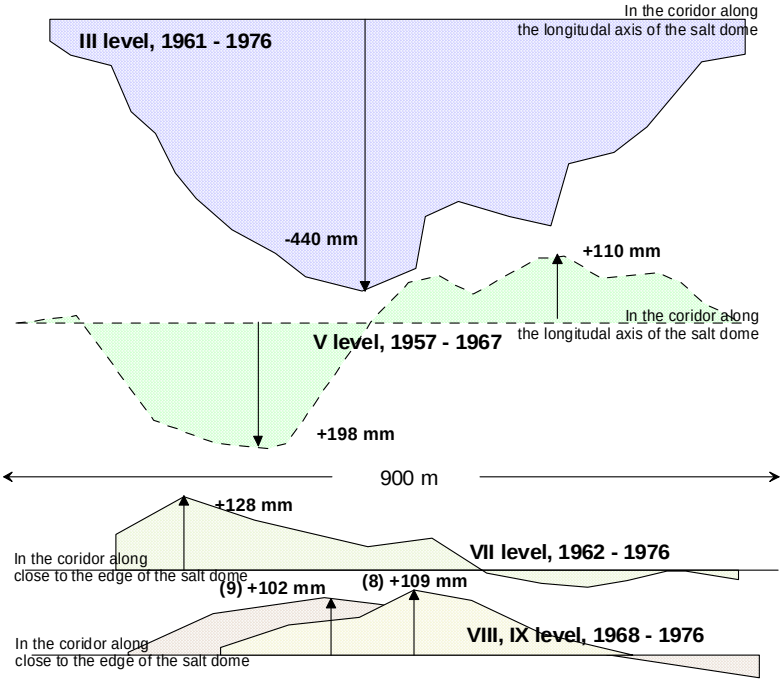

Fig. 2. Profiles of the vertical displacements of levels in the Wapno Salt Mine (Kortas, 2008)

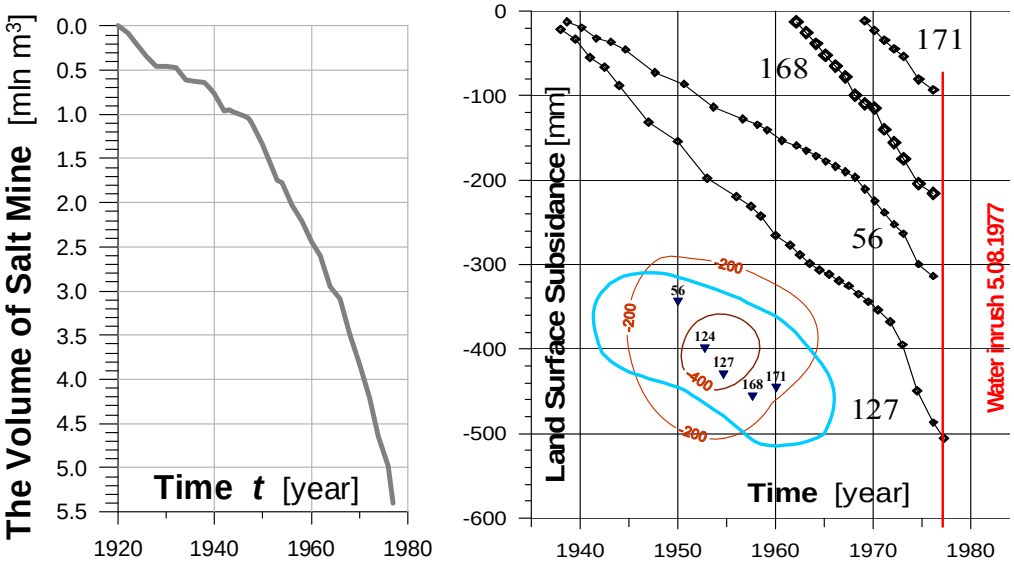

Fig. 3. The volume of the Wapno Salt Mine and the land subsidence in 1937-1977 [mm]

The boundaries of the formations that are different in respect of deformability constitute special places in the rock mass undergoing deformation. That is where we can expect the occurrence of extreme stresses, followed by cracking and slides that develop during the deposit formation and movements caused by the influence of workings. In the case of salt domes, the places like that include vertically arranged formations of anhydrite and the adjacent K-Mg salt layers which are more rigid than regular salt deposits. Owing to the water hazard, the most dangerous is the occurrence of tensile strains in the direction which is normal in respect of layer planes. The locations of the vertical layers containing anhydrite at Level III of the Wapno Salt Mine are shown in Fig. 4.

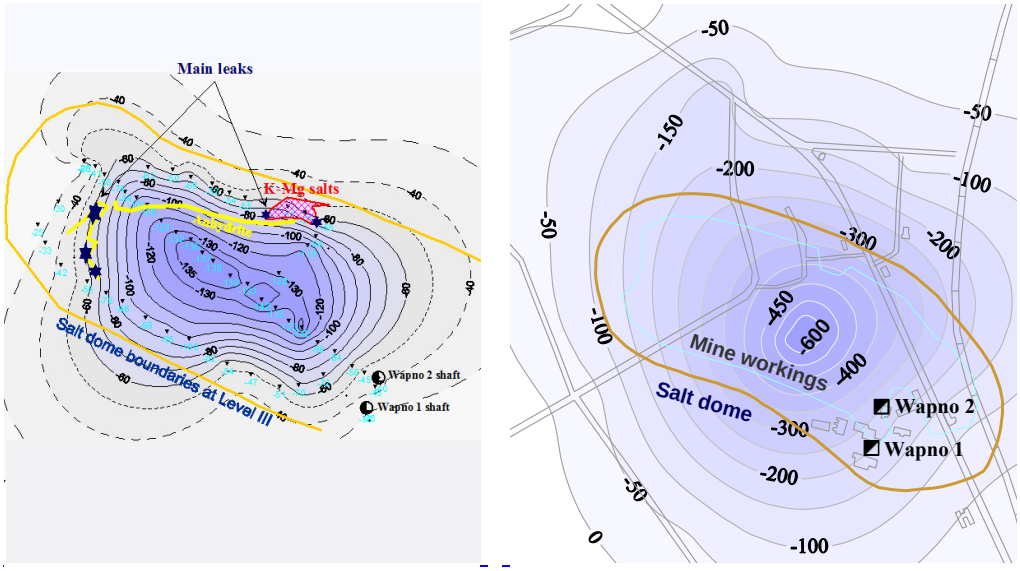

Fig. 4. Subsidence at Level III of the Salt Mine in 1973-1976, with the locations of the vertical layers of anhydrite and K-Mg salts (left), and land surface subsidence in 1937-1976 (right)

Close to anhydrite layers, brine leaks appeared, first at Level IV and later at Level III. The presence of surface water markers was identified in such leaks. The leaks occurred first at the SW and NE boundaries of the salt dome, and, in recent weeks before the inflow of water into the mine, they were developing in the working zone, along the line of anhydrite and K-Mg salt interlayers. The increase of inflow, with concurrent decrease of salt concentration, led to the catastrophic inrush of water into the salt mine on 5 August 1977 (Ślizowski & Kortas, 1980). Several small sink-holes, caused by dewatering of the salt dome cap, appeared already within the first 24 hours, followed by a large land subsidence developing close to the NE salt dome wall, within several months (Figs. 5 and 6). More than 0.3 million cubic metres of liquefied clay and sand materials were transported from the salt dome surroundings into the mine workings and forty buildings were destroyed or damaged.

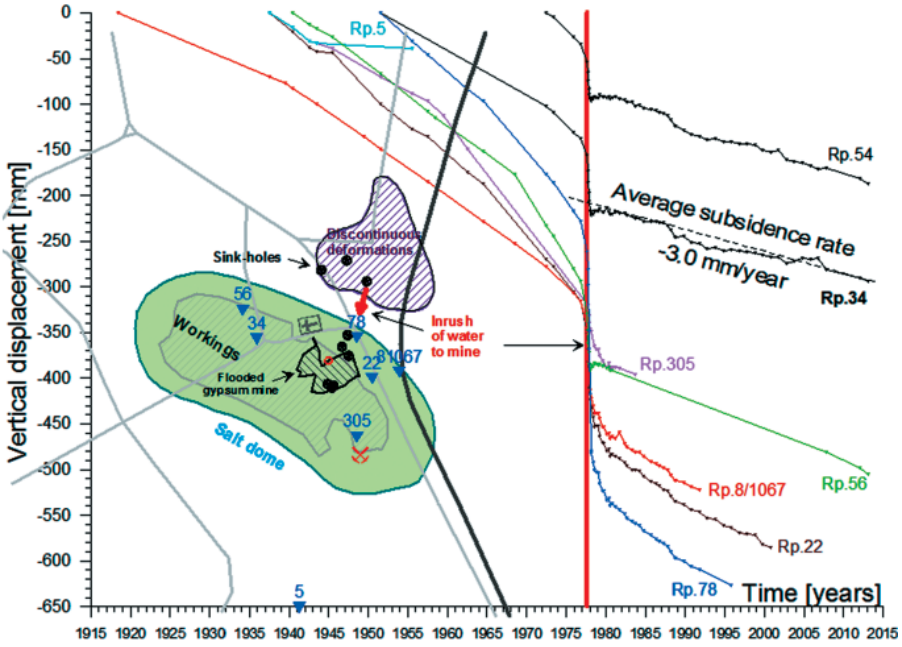

Fig. 5. Land surface subsidence in Wapno before and after water inrush into the Salt Mine in 1977 (Maj, in: Rasała, 2014)

Fig. 6. A sink-hole in Wapno

Considering the above-mentioned geological and mining conditions, as well as the indications of the influence of salt extraction on rock mass and land surface, the question arises whether the mine workings' effects could have caused such significant horizontal tensile strain within the protection shelf to allow for the contact of water from the salt dome cap with the mine's workings, leading to flooding.

2. Research Method

2.1. Modelling Simplifications

When the roof protection shelf and the boundary pillars are tight, deformations and cracks occurring inside the salt dome do not cause any direct water hazard to the salt mine. It is claimed, however, that the roof protection shelf cracking is the cause of numerous inflows of water into the diapir salt mines (e.g. Spackeler, 1953). In order to determine the boundary of safe deformations in the roof protection shelf, A. Sałustowicz considered the dependence of the bending of an elastic beam loaded with mass forces (Sałustowicz et al., 1962), however, omitting rheological viscous properties of salt rocks. By the end of the 20th century, we obtained a possibility of numerical determination of the time-dependent stresses, strains, and displacements in an elastic-viscous medium (e.g. Filcek et al., 1994; Kortas, 2008; Munson, 1997; Munson & Dawson, 1984; Ślizowski, 2006; and Ślizowski & Urbańczyk, 2004). In such numerical calculations, the transformation of the geological rock mass and the geometrical salt-mine complexity require the construction of 3D models in which the number of elements is considerably larger than 10^6. The consideration of the time of workings' excavation in elastic-viscous medium models causes the repetition of even several hundred-step cycles of calculations after each change of the salt mine's geometrical structure. Since the calculation time of a single step takes a dozen or several dozens of minutes and time increases exponentially with the number of elements, the calculation time cycle takes many weeks for each single task. Consequently, it is necessary to introduce simplifications in geometrical and physical assumptions. That is the case especially when we look for the physical model parameters under multi-task model studies by comparing calculation results with measurement results.

Considering the object of study concentrating on the condition of the protection rock salt body, the accuracy of the geometrical model of the working zone is not a primary goal. Some parts of the salt mine space, e.g. particular salt extraction levels, can be replaced by an equivalent medium, with appropriately changed parameter values. What is the condition of such replacement, however, is the geometrical and physical similarity of the repeating parts of the room-and-pillar structure of the particular level and the assignment of continuity to the area of the structure being homogenized, using appropriate equivalent properties. Proceeding in a similar way, we usually apply homogenization to replace the lithological complexity of rock masses.

The homogenization method of the extraction area and the room-and-pillar structure in a salt dome was introduced for the first time in 2011. A 2D+t elastic-viscous model was used to determine the behaviour of the mining field's surroundings in the Kłodawa Salt Mine (Kortas & Maj, 2012). In the research project discussed in the present study, time-dependent homogenization of the salt mine space in a 3D+t elastic-viscous model was applied for the purpose of simulation and determining the deformations of the roof protection shelf in the Wapno Salt Mine.

2.2. Physical Model

Current world literature uses Hooke's constitutive model, with Norton-Bailey's power creep law (Bailey, 1929; Norton, 1929) to salt medium as a standard. Hooke's law of linear elasticity can be recorded in the form of two tensor equations, binding stress with strain, where the first one describes the rule of shape change and the second one the rule of volume change:

$$ {}^{D}\varepsilon_{ij} = (1+\nu)/E\ {}^{D}\sigma_{ij}; \qquad {}^{A}\varepsilon_{m} = (1-2\nu)/E\ {}^{A}\sigma_{m} \tag{1}$$

where:

$ {}^{D}\varepsilon_{ij} = \varepsilon_{ij} - {}^{A}\varepsilon_{m}\delta_{ij}$ (δ_{ij} — Kronecker's delta) is the strain deviator,
$ {}^{D}\sigma_{ij} = \sigma_{ij} - {}^{A}\sigma_{m}\delta_{ij}$ — the stress deviator,
$ {}^{A}\varepsilon_{m} = 1/3(\varepsilon_1 + \varepsilon_2 + \varepsilon_3)$ — the mean strain,
$ {}^{A}\sigma_{m} = 1/3(\sigma_1 + \sigma_2 + \sigma_3)$ — the mean stress,
E — Young's modulus, and
ν — Poisson's ratio.

We have applied Norton-Bailey's power creep law for the purpose of simulation and viscous medium behaviour study, as determined by the following equation:

$$\dot{\varepsilon}_{ij} = \frac{3}{2} mA \exp[-Q/(RT)]\sigma_{ef}{}^{n-1}\sigma_{ij}t^{m-1} \tag{2}$$

where:

Q — is the activation energy,
R — gas constant,
T — Kelvin temperature, and
A, n, m — material constants.

The function of A, Q and R material constants determines the compliance of material to creep B, in particular temperature T, as expressed by the formula:

$$B = A\exp[-Q/(RT)] \tag{3}$$

The Huber-Mises-Henky effective stress σ_{ef} was determined by the formula:

$$\sigma_{ef} = \frac{1}{\sqrt{2}}\sqrt{(\sigma_{11}-\sigma_{22})^2 + (\sigma_{22}-\sigma_{33})^2 + (\sigma_{33}-\sigma_{11})^2} \tag{4}$$

The stress tensor components in the main directions of $\sigma_{11}, \sigma_{22}, \sigma_{33}$ are recorded as $p_1 > p_2 > p_3$ in the present study. In the hydrostatic state of stress which occurs in salt rocks before salt extraction: $p_1 = p_2 = p_3$, or $\sigma_{ef} = 0$.

2.3. Homogenization Parameters

In either natural or technical processes, elastic and viscous deformation properties of materials can change under physical or chemical influences. Since in the case of a medium subjected to the power creep law in constitutive equations multiplication, division, raising to a power or

logarithming correspond to addition, subtraction, multiplication, and division, it is comfortable to determine property changes with logarithmic functions. Let the value of β determine the power change of the viscous properties from ${}^1B$ to ${}^2B$:

$$\beta = \log({}^2B / {}^1B) \tag{5}$$

where B is the creep compliance and β is the increase of the creep compliance factor, ${}^2B > {}^1B$ and $\beta > 0$.

Similarly, we can define the value of η, as an power change of the bulk modulus $K = E/[3(1 - 2\nu)]$. For the established value of Poisson's ratio ν, that would be limited to the change of the Young's modulus E:

$$\eta = \log({}^2K / {}^1K) = \log({}^2E / {}^1E) \quad \text{for} \quad \nu = \text{const} \tag{6}$$

where η is the reduction of the bulk modulus, ${}^2K < {}^1K$ and $\eta < 0$.

In such formulation, the values of η and β are the parameters of the medium sensitivity to the factor that is responsible for the volumetric and shape changes of the medium. For example, humidification or drying, cracking or perforation, and also mechanical degradation of pillars and shelves or of their complexes can be such factors. The homogenization parameters of the Wapno Salt Mine levels, resulting from perforation and degradation, were established by our model studies, with the condition of their compliance with the observed displacements.

3. Course of Research

In our research, we applied a geometric model in the form of a cuboid, with the horizontal dimensions of 1900 m × 1350 m and the height of 1000 m. In the X and Y axial directions, the salt dome had the dimensions of 900 m × 350 m, and the dimensions of the salt mine's structure were 800 m × 250 m. The structure's space included the levels, from Level III on the vertical level ordinate of that roof, Z = –359 m, to the floor of Level IX, at the depth of 543 m. A protection salt shelf was preserved over Level III, from the depth of 359 m to 160 m, with the salt dome cap above it, to the depth of 10 m. Above the cap, Quaternary overburden was laid up to the land surface (Z = 0 m). The surrounding formations were located outside the salt dome boundaries.

Four Areas were distinguished in the workings' zone: (1) – from the floor of the roof protection shelf to the floor of Level III at the depth of 384 m, (2) – from the floor of Level III to the floor of Level IV at Z = –405 m, (3) – Levels V and VI down to the depth of 454 m, and (4) – Levels VII-IX down to the depth of 543 m. The properties of particular formations were assumed to be those specified in the 2008 study (Kortas, 2008): for $n = 2$ and m = 1. The parameters β, η of Areas 1-4 were different in each ten-year period.

Assuming a symmetry in vertical planes run along axes X and Y of the salt dome, the geometrical model was reduced to $^1/_4$ of the 3D space (Fig. 7, left). Displacement boundary conditions were assumed (Fig. 7, left), and the hydrostatic state of initial stress (Fig. 7, right) was obtained by simulation of the rock mass creep process, without consideration of workings, in the years t = –5000 to 0. For salt rocks, the following were assumed: Young's modulus E = 15 GPa, Poisson's ratio: ν = 0.3, and the creep compliance $B = 5^*10^{-25}$ Pa^{2}s^{-1}.

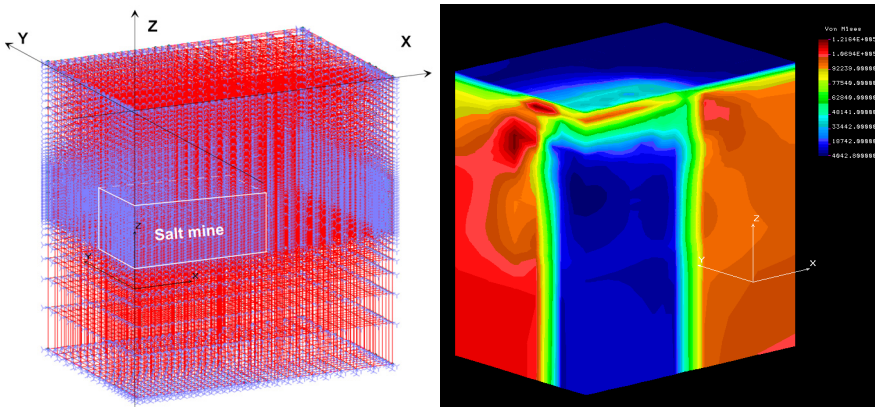

Fig. 7. A $^1/_4$ model of the salt dome, with the location of the salt mine and the boundary conditions (left), as well as the initial distribution of effective stresses (right)

A series of preliminary model studies was designed to determine the influence of the parameter $\eta(E) \in [-0{,}25; -0{,}50; -1{,}00; -1{,}50; -2{,}00]$ on land surface subsidence, at the constant value of the parameter b(B) = 0. In that series of studies, the parameters did not change in time, but they were different in particular tasks. The simulation results are represented by the maximum land subsidence in the function of time ${}^P w_{\max}(t,\eta)$ at the crossing point of symmetry planes. The results obtained are approximated by a bunch of power functions shown on Fig. 8.

In the subsequent series of tasks, the influence of the concurrent h and b on the land subsidence ${}^P w_{\max}(t)$ was tested. An example of results obtained is illustrated by the graph shown in Fig. 9. After immediate subsidence as a result of elastic reaction, creep occurred, and that is described by the power functions of time.

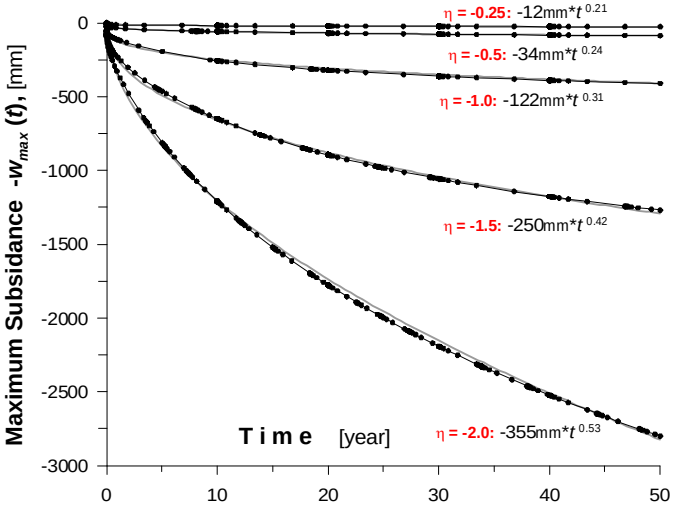

Fig. 8. Correlations of $w(t)$ at $\eta(E) \in [-0{,}25; -0{,}50; -1{,}00; -1{,}50; -2{,}00]$

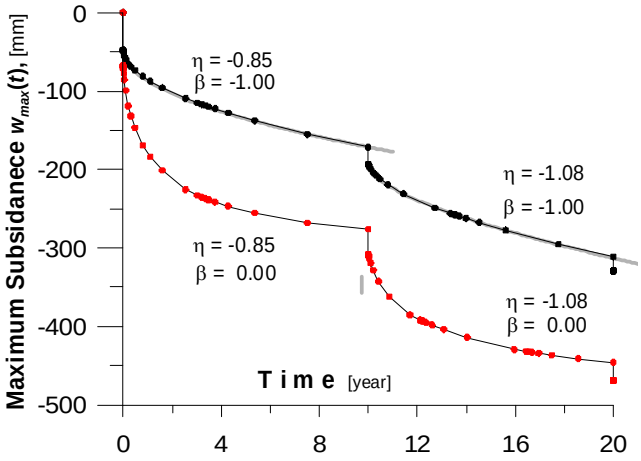

Fig. 9. The influence of η and β parameters on the function $w_{\max}(t)$

After preliminary test series, the compliance between the model displacements ${}^{P}w_{\max}(t)$ and those observed on the land surface above the Wapno Salt Mine was obtained. Subsequent test series were designed to obtain compliance of a sequence of vertical displacements values at the particular salt mine levels $[{}^{K}w_{\max}(t)]$ and on the land surface ${}^{P}w_{\max}(t)$. The tests are illustrated by two graphs presented in Fig. 10.

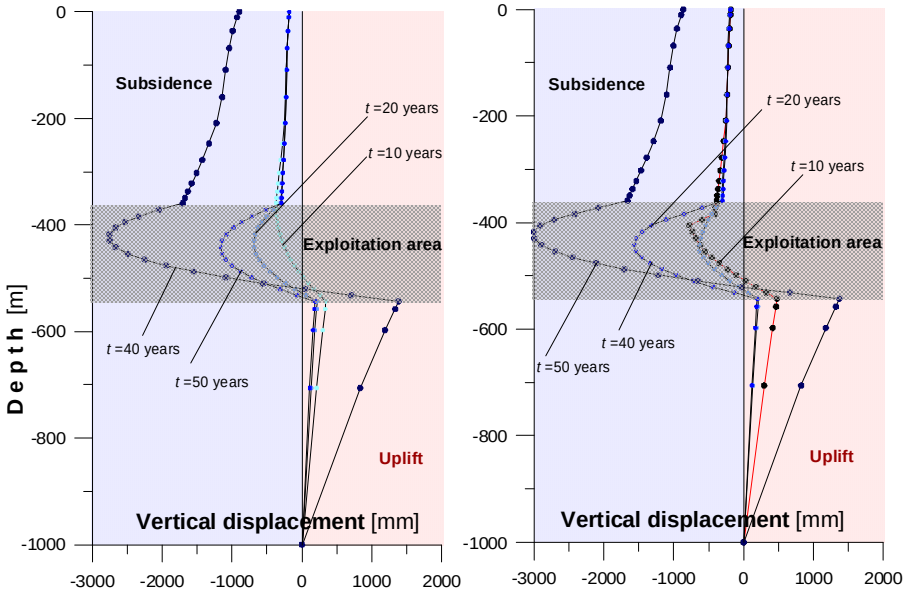

Fig. 10. The dependence of maximum vertical displacements on depth, with η and β parameters being constant (left) and changing in time (right)

The largest subsidence values occurred in the centre of Levels III and IV of the salt mine, with the largest uplifts at lower Levels IX and VIII. The final result of that stage of studies included proper diversification of the homogenization η and β parameters for particular salt mine areas that are changeable in time. Fig. 11 presents the graphs of extreme model displacements in the function of time, corresponding to the results of the measurements conducted in the salt mine and on its land surface.

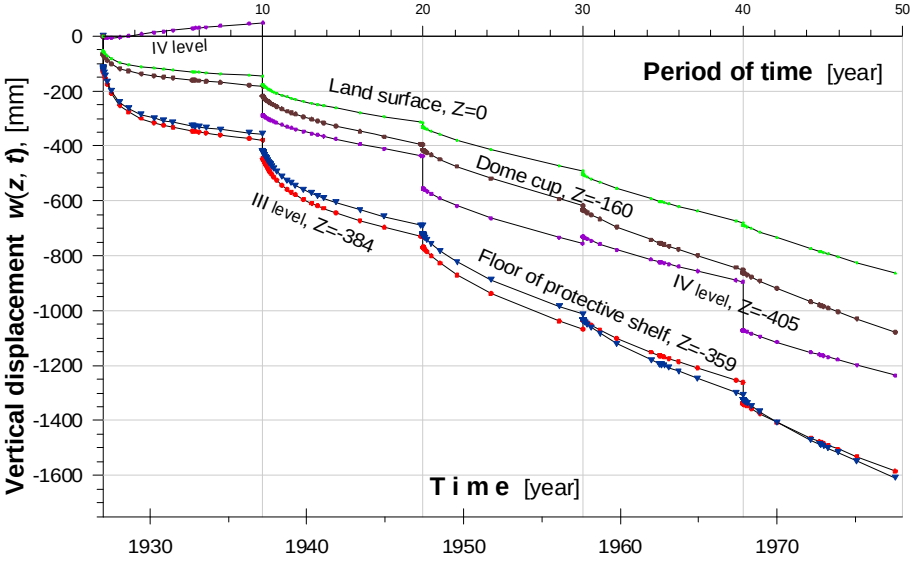

Fig. 11. Subsidence of land surface and of upper salt mine's levels

At the beginning, until year 30 (upper horizontal axis), the largest subsidence occurred at the floor of Level III, followed by that at the floor of the protection shelf. In a later period, Level III was converging and, consequently, the floor of the protection shelf was subsiding. Vertical displacements of the horizon $Z = -160$ m (the roof of the protection shelf) were significantly lower. The calculated difference between the shelf floor and roof increased with time, and it amounted to +553 mm in year 50. For that reason, the average deformation of the protection shelves in the vertical direction, equal to: 553 mm / 199 m = +2.8 mm/m, constituted expansion. Land surface subsidence in year 50 reached the value of –872 mm (Fig. 11). At the lower Level IX, uplifts occurred, reaching up to +1435 mm in year 50. In the next chapter, the results of the analysis of stress and strain in the roof protection shelf are presented.

4. Results of the Model Studies Concerning the Roof Protection Shelf Deformation

The analysis of the calculation results, obtained from the model studies, indicated that expansion stresses appeared in three locations: the largest ones on the border of the boundary pillars

and the salt dome surroundings and lower ones within the salt dome cap and the roof protection shelf. The distribution of the maximum main stress p_1 is presented in Fig. 12. After ten years, the maximum stress p_1 within the salt dome cap reached the value of +0.06 MPa, and increased to +5.3 MPa after 30 years; however, the three main stress components reached the values of p_1 = +7.8 MPa, p_2 = +5.1 MPa, and p_3 = +3.7 MPa in year 50. Similarly to the salt dome cap, the three main stresses were expanding also in the roof shelf, and the maximum stress reached the value of p_1 = +5.1 MPa in year 50.

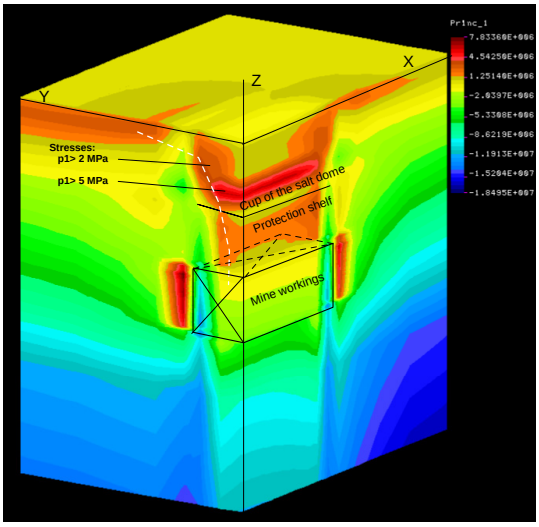

Fig. 12. The maximum stresses p_1 [Pa] after 50 years, with salt mine workings locations

The maximum values of tensile strain occurred in the roof protection shelf. They were not significant initially but they were increasing in proportion to the expansion stresses which were increasing with time. The maximum values of the strain components in the horizontal plane of the roof protection shelf occurred in the direction of the salt dome's shorter axis Y. The strain distribution is presented in vertical and horizontal cross-sections in Figs. 13-15 (the graphs contain identification indices and colours in the deformation units, or 1 = 1000‰).

The maximum strain ${}^{\max}\varepsilon_y$ occurred in the central part of the roof protection shelf at the depths from 220 to 260 m and at the distance of 100 m from the vertical axis Z. The maximum deformation reached the value of +2.5‰ after ten years from the commencement of salt extraction, and it increased to +3.8‰ in year 30, and to +4.6‰ in year 50.

5. Rock Mass and Land Surface after Inrush of Water into the Wapno Salt Mine

Opening of the water flow paths caused uncontrolled and increased leaching of salt in the roof protection shelf. After the inflow of water into the salt mine, the protection pillars and shelves

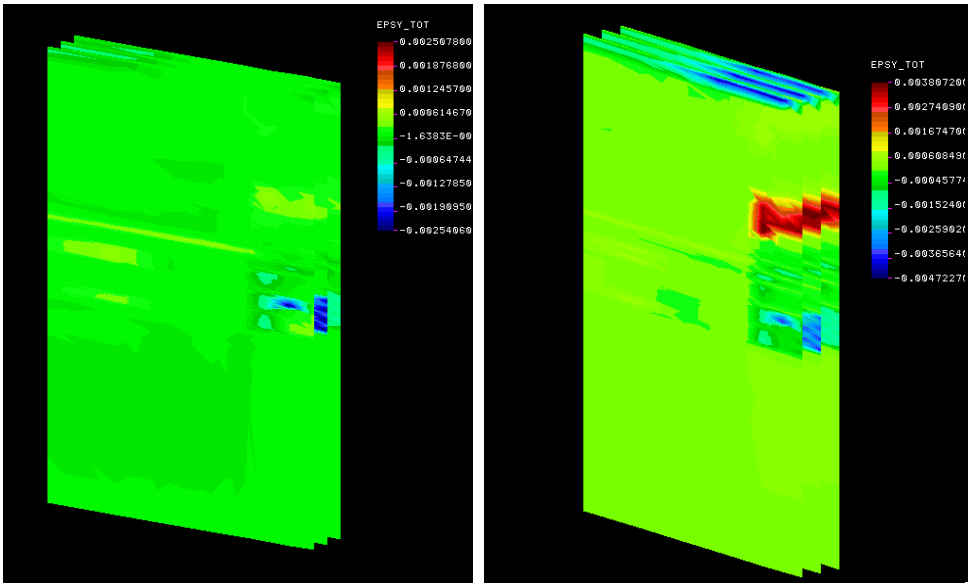

Fig. 13. Distribution of the horizontal strain ε_y in the roof protection shelf,in vertical cross-sections; X ∈ [1000, 1050, 1100 m] after 10 (left) and 50 years (right)

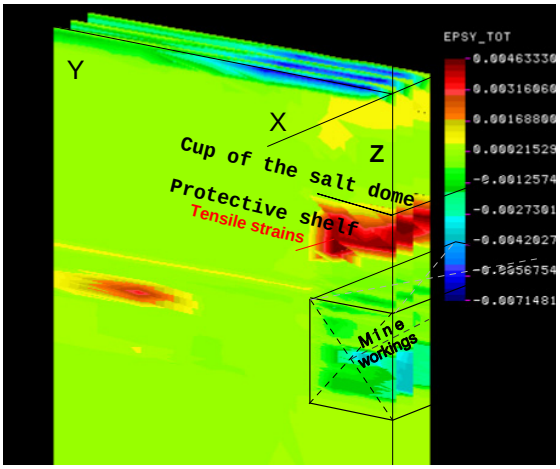

Fig. 14. Distribution of the strain ε_y after 50 years in the roof shelf, in vertical cross-sections; X ∈ [1000, 1050, 1100 m], $^{max}\varepsilon_y$ ∈ [+4.6‰, +3.6‰, +2.9‰]

were being leached, at first at the upper levels, next at the lower. After certain time, the filling of workings with brine under hydrostatic pressure led to the relaxation of effective stresses and the reduction of tensile strain in protection pillars and shelves between rooms. The results of survey indicated the changing rates of land subsidence.

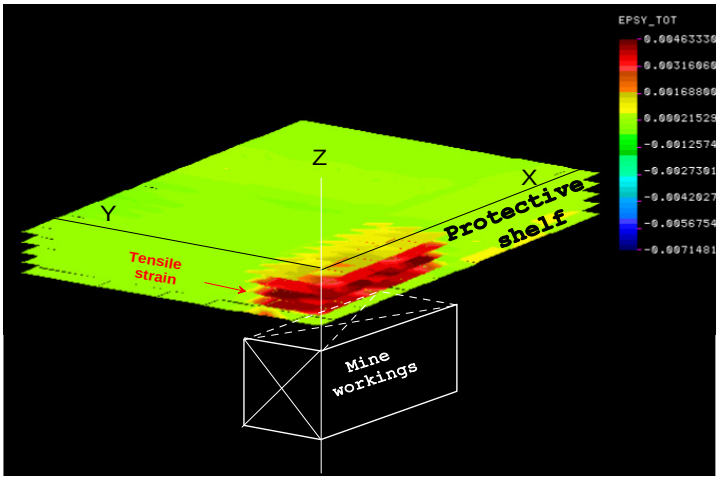

Fig. 15. Locations of the maximum horizontal strain $^{max}\varepsilon_y$ after 50 years, in horizontal cross-sections; Z ∈ [–220, –260 and –300 m], Max[$^{max}\varepsilon_y$(H)] = +4.64‰

Another series of model studies, with the variation of the homogenization parameters b and h, was intended to obtain the compliance of the numerical calculation results with those of actual land surface levelling measurements obtained after the salt mine had been flooded. Simulation results are shown in Fig. 16.

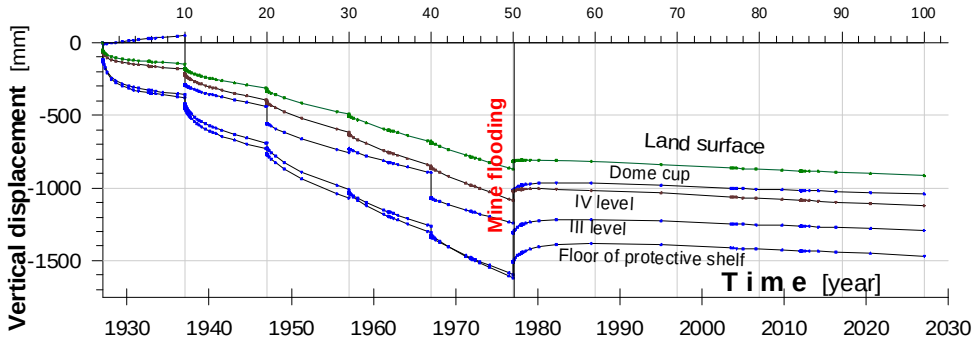

Fig. 16. Model vertical displacements of points within the salt dome

During mining operations, from 0 to 50th year the results of the model calculations showed the average rate of maximum land surface subsidence of –16.6 mm/year, while after the flooding of workings in 1977-1978 (after 50 years), the rate was reduced primarily down to –7 mm/year, to keep decreasing in the subsequent forty years down to –2 mm/year. The flooding of workings caused initially a land surface uplift, changing into subsidence after several years, also observed in measurement results (see Fig. 5).

After the workings had been flooded, it was not possible to take any measurements inside the salt mine. Flooding simulations indicated that the roof of protection shelf was raised by maximum +65 mm, and the floor of protection shelf by +113 mm in year 50. We should mention that, after a controlled filling of lower levels of the Solno Salt Mine in Inowrocław with brine, uplifting of the highest level to the value of +81 mm (Kortas, 1997) was observed, and after the flooding process completion, land surface uplifts by maximum +6 mm were identified. Land surface observations conducted after the Wapno Salt Mine flooding indicated that, after short-term several millimetre uplifts found in 1978, land subsidence continued, with the largest one identified in the discontinuous deformation zones outside the salt dome area (see Fig. 5).

6. Analysis of Results and Conclusions

Our model studies allowed us to appraise the tensile strains that were increasing under the influence of salt extraction, within the roof protection shelf located above the workings of the Wapno Salt Mine. The strain components in the horizontal and vertical directions were the tensile strains, increasing with the spatial development of the salt mine.

The occurrence of omnidirectional tensile stresses in the protection rock salt body are the signals of hazardous geomechanical conditions, owing to the possibility of deformation propagation, allowing for the inflow of water into the salt mine. Laboratory studies indicated that a uniaxial tensile strength of rock salt is close to 0.5 MPa (Dreyer, 1972), and the corresponding critical strain for the Young's modulus $E \geq 1$ GPa complied with the conditions of the uniaxial strain $\varepsilon \leq + 0.5‰$. Therefore, the roof shelf deformations, obtained from our model and the extraction process simulation, exceeded a safe critical strain already after ten years, and continued to increase up to +5.1‰.

We should add that, during the halokinetic process of salt dome uplift, fractures were developing at the contact planes of salts that were susceptible to creep and the rigid formations, also close to the salt dome boundary. Such fractures could be filled with syngenetic fluids. Excessive deformation of the central part of the protection shelf was not the cause of water inflow into the salt mine but rather the cause was the propagation of that deformation in the protection shelf or, which is more probable, the opening of previously existing fractures during shelf expansion. The opening of fractures within the shelf subjected to deformation, from the caprock into the workings, allowed for water infiltration, followed by leaching out of migration paths, and that led to final salt mine flooding.

We should also point out here the simulation results indicating the appearance of tensile stress zone, within the salt dome cap and under-surface formations outside the salt dome's contour in the direction of the shorter axis Y.

In the case of opening of the flow paths across boreholes made in the boundary pillars, the mining practice relies on plugging the boreholes and damming the leak area. However, no open fractures in the roof shelves with water infiltration could have been controlled in any salt mine yet. The appearance of a number of new leaks at Level III of Wapno Salt Mine, along WE direction, was an indication of the flow path propagation, observed by the author in July 1977. That happened within several weeks before the water inrush into the salt mine. Initially, the humidification of the room roofs increased, followed by brine "rainfall" and rooms' floors flooding. A system of fractures, fissures, and leaching area was moving from the west to the east edge of

the salt dome. Owing to faster solubility of the vertical K-Mg salt layers, existing at the east edge of salt dome, favourable conditions existed for extensive leaching processes, followed by the transport of liquefied sand and silt material from the salt dome surroundings into the workings, and in consequence for the development of a large subsidence.

Omnidirectional tensile stresses in the roof protection shelf, found in the geomechanical model, the identification of considerable tensile strains in the central part of the roof protection shelf, and the occurrence of maximum values of strain in the direction being parallel to the shorter salt dome axis confirm the opinion that the geomechanical conditions evoked by the workings' effects constituted essential causes of the water hazard increase and, consequently, of the salt mine's catastrophic flooding. We should add that the exploitation commenced at Level X and the preparation of Levels XI and XII for that purpose, was mining mistake. In the similar conditions of other multi-level room-and-pillar salt mines, salt exploitation will lead to the occurrence of positive values of stresses and tensile strains, favouring the opening of fractures within the protection shelf. That was also demonstrated by the studies presented in the paper by Kortas and Maj (2012).

The method of room-and-pillar structure homogenization was first introduced in a 2D+t geometric model (Kortas & Maj, 2012). The present publication concerning a 3D+t model opens new possibilities of applying physical elastic-viscous medium models to determine the changes in time in the distribution of the displacements and strains inside the rock mass and on the land surface.

References

Bailey R.W., 1929. Trans. World Power Conf. Tokyo. p. 1089.

Dreyer W., 1972. *The science of rock mechanics. Part 1. The strength properties of rocks*. Series on Rock and Soil Mechanics, Vol. 1, No. 2. Trans. Tech. Publications.

Filcek H., Walaszczyk J., Tajduś A., 1994. *Metody komputerowe w geomechanice górniczej*. Śląskie Wydawnictwo Techniczne. Katowice.

Kortas G., 1979. *Ruch górotworu przed wdarciem się wód do wyrobisk kopalni soli w Wapnie*. Ochrona Terenów Górniczych, nr 49. Katowice.

Kortas G., 1997. *Zachowanie się górotworu w kopalni soli Solno*. Przegląd Górniczy, nr 6.

Kortas G., 2007. *The influence of the form of a salt mine on the displacement of the ground surface*. Arch. Min. Sci., Vol. 52, No 1, p. 107-120.

Kortas G. (red.), 2008. *Ruch górotworu w rejonie wysadów solnych*, Wyd. IGSMiE PAN. Kraków.

Kortas G., Maj A., 2005. *Evaluation of stresses around an underground reservoir of liquid fuels in unrecognised mining and geological conditions*. A.A.Balkema Publishers, Pocc.Int. Symp. ISRM Eurock, Brno.

Kortas G., Maj A., 2012. *Warunki geomechaniczne w caliznach chroniących przed wodami, na przykładzie kopalni soli Kłodawa*. Przegląd Górniczy, nr 12.

Munson D. E., 1997. *Constitutive Model of Creep in Rock Salt Applied to Underground Room Closure*. International Journal of Rock Mechanics and Mining Sciences & Geomechanics, Vol. 34, Iss. 2, s. 233-247.

Munson D.E., Dawson P. R., 1984. *Salt Constitutive Modeling using Mechanism Maps*. Proc. 1st Conf. on the Mechanical Behavior of Salt, Trans Tech Publications. Clausthal-Zellerfeld. Germany.

Norton F.H., 1929. *The creep of steel at high temperatures*. McGraw-Hill. New York.

Rasała M. (red.), 2014. *Dokumentacja geologiczna określająca zagrożenia terenu pogórniczego kopalni soli Wapno w zakresie określenia jego przydatności do zagospodarowania i rewitalizacji*. Hydro-Nafta, UAM. (praca niepublikowana).

Sałustowicz A., Dziunikowski J.L., Hwałek S., 1963. *Wytrzymałość górotworu przy eksploatacji złoża solnego komorami poziomymi i pionowymi*. Państwowa Rada Górnictwa PAN. SITG. Katowice.

Spackeler G., 1953. *BergbauKunde Leberbrief*. Verl. Technik. Berlin.

Ślizowski J., 2006. *Geomechaniczne podstawy projektowania komór magazynowych gazu ziemnego w złożach soli kamiennej*. Studia. Rozprawy. Monografie Nr 137. Wyd.IGSMiE PAN. Kraków

Ślizowski J., Urbańczyk K., 2004. *Influence of depth on rock salt effort around the single chamber*, Wyd. IGSMiE PAN. Kraków.

Ślizowski J., Urbańczyk K., 2012. *An attempt asses suitability of Middle-Poland salt domes for natural gas storage*. Arch. Min. Sci., Vol. 57, No 2, p. 335-349.

Ślizowski K., Kortas G., 1980. *Zagrożenie powierzchni spowodowane eksploatacją wysadów solnych na przykładzie Kopalni Soli im. T. Kościuszki w Wapnie*. Ochrona Terenów Górniczych, nr 51.

Tajduś K., 2013. *Numerical simulation of underground mining exploitation influence upon terrain surface*. Arch. Min. Sci., Vol. 58, No 3, p. 605-616.

Received: 23 May 2014